



**Michigan
Technological
University**

Michigan Technological University
Digital Commons @ Michigan Tech

Michigan Tech Publications

6-12-2020

Visual feature extraction from dermoscopic colour images for classification of melanocytic skin lesions

Walid Al-Zyoud
German Jordanian University

Athar Abu Helou
German Jordanian University

Eslam AlQasem
German Jordanian University

Nathir A. Rawashdeh
Michigan Technological University, narawash@mtu.edu

Follow this and additional works at: <https://digitalcommons.mtu.edu/michigantech-p>



Part of the [Computer Sciences Commons](#)

Recommended Citation

Al-Zyoud, W., Helou, A., AlQasem, E., & Rawashdeh, N. (2020). Visual feature extraction from dermoscopic colour images for classification of melanocytic skin lesions. *EurAsian Journal of BioSciences*, 14, 1299-1307.

Retrieved from: <https://digitalcommons.mtu.edu/michigantech-p/14695>

Follow this and additional works at: <https://digitalcommons.mtu.edu/michigantech-p>



Part of the [Computer Sciences Commons](#)



Visual feature extraction from dermoscopic colour images for classification of melanocytic skin lesions

Walid Al-Zyoud ^{1*}, Athar Abu Helou ¹, Eslam AlQasem ¹, Nathir A. Rawashdeh ²

¹ Department of Biomedical Engineering, German Jordanian University, Amman, JORDAN

² Department of Applied Computing, College of Computing, Michigan Technological University, USA

*Corresponding author: walid.alzyoud@gnu.edu.jo

Abstract

The early diagnosis of Melanoma is a challenging task for dermatologists, because of the characteristic similarities of Melanoma with other skin lesions such as typical moles and dysplastic nevi. **Aims:** This work aims to help both experienced and non-experienced dermatologists in the early detection of cutaneous Melanoma through the development of a computational helping tool based on the "ABCD" rule of dermoscopy. Moreover, it aims to decrease the need for invasive biopsy procedure for each tested abnormal skin lesion. **Methods:** This is accomplished through the utilization of MATLAB programming language to build a feature extraction tool for the assessment of lesion asymmetry, borders irregularity, and colors variation in the tested lesion. **Results:** The helping tool obtained a sensitivity of 81.48%, a specificity of 52.83% and accuracy of 62.50% in the assessment of the Asymmetry Index. A new metric for the borders irregularity index was built. Finally, for the Colors Variation Index algorithm a sensitivity of 51.37%, a specificity of 61.51% and accuracy of 57.80% was achieved. **Conclusions:** This work created a computational tool based on the ABCD-rule, which is helpful for both experienced and non-experienced dermatologists in the early discrimination of Melanoma than other types of skin lesions and to eliminate the need of the biopsy procedure. A new metric for the Borders Irregularity Index was established depending on the number of inflection points in the lesion's borders.

Keywords: computational assessment, melanocytic skin lesions, ABCD rule, dermoscopy

Al-Zyoud W, Abu Helou A, AlQasem E, Rawashdeh NA (2020) Visual feature extraction from dermoscopic colour images for classification of melanocytic skin lesions. *Eurasia J Biosci* 14: 1299-1307.

© 2020 Al-Zyoud et al.

This is an open-access article distributed under the terms of the Creative Commons Attribution License.

INTRODUCTION

Several image acquisition techniques have been reported for skin lesion inspection and Melanoma recognition, starting from the commercial digital cameras that reproduce images of what the clinicians see with the naked eye (Day and Barbour 2000), but the resulted images are poor in resolution-making a more in-depth inspection of the lesion impossible (Loane et al. 1997). It is a challenging task for dermatologists to discriminate Melanoma from other types of skin lesions, even with the use of the different medical algorithms such as the ABCD rule and the 7-point checklist.

The ABCD rule which is also known as STOLZ's algorithm that was developed by Stolz *et al.* (1994); is a scoring system used to classify the benign melanocyte lesions from Melanoma lesions, depending on four different characteristics of the lesion: (A)asymmetry, (B)border, number of (C)colors, and number of (D)dermoscopic structures. As described in **Table 1**,

each characteristic is quantitatively scored based on specific criteria, which are then scaled empirically by weight factors indicating determined importance.

The summation of these weighted scores yields the *total dermoscopy score* or TDS, as shown in the equation below (Stolz et al. 1994).

$$TDS = 1.3 A_{score} + 0.1 B_{score} + 0.5 C_{score} + 0.5 D_{score} \quad (\text{Eq.1})$$

Based on the TDS score, a lesion is diagnosed as Melanoma if the TDS is higher than 5.45 and is considered suspicious if its TDS is in the range 4.8-5.45. More clarification and examples in attaining the TDS are shown in **Fig. 1**.

The automated classification of skin lesions have been proposed for Melanoma detection; they have a generic sequence of steps that include: **image**

Received: November 2019

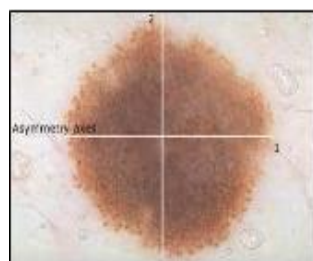
Accepted: April 2020

Printed: June 2020

This work created a computational tool based on the ABCD-rule, which is helpful for dermatologists in early discrimination of Melanoma to eliminate a need for biopsy. A new metric for the Borders Irregularity Index was established depending on the number of inflection points in the lesion's borders.

Table 1. Criteria of ABCD rule of dermoscopic images

Criterion	Description	Score	Weight
Asymmetry	In 0, 1 or 2 axes; assess contour and colors and structures.	0-2	1.3
Border	The abrupt ending of pigment pattern at the periphery, in 0-8 segments.	0-8	0.1
Color	Presence of up to 6 colors 1-6 (white, red, light-brown, dark-brown, blue-gray, and black).	1-6	0.5
Dermoscopic structures	Presence of network, structure-less or homogeneous areas, streaks, dots, and globules.	1-5	0.5



$$A = 0 \times 1.3 = 0;$$

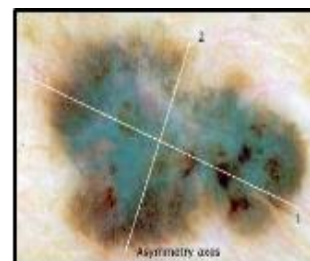
$$B = 8 \times 0.1 = 0.8$$

$$C = 2 [\text{light-brown, dark-brown}] \times 0.5 = 1;$$

$$D = 2 [\text{network, globules}] \times 0.5 = 1;$$

$$\text{TDS} = 2.8$$

a) Benign



$$A = 2 \times 1.3 = 2.6;$$

$$B = 5 \times 0.1 = 0.5;$$

$$C = 4 [\text{light/dark-brown, blue-gray, black, white}] \times 0.5 = 2;$$

$$D = 4 [\text{homogeneous areas, streaks, dots, globules}] \times 0.5 = 2;$$

$$\text{TDS} = 7.1$$

b) Melanoma

Fig. 1. Example of the ABCD rule (Argenziano et al. 2000)

preprocessing, lesion segmentation, feature extraction, and lesion classification (Jain et al. 2015, Oliveira et al. 2018).

This work aims to help in the early detection of cutaneous Melanoma through the development of a helping tool based on the ABCD rule that profoundly depends on the dermoscopic images to extract features for two purposes to decrease the need for the biopsy procedure for each abnormal tested lesion.

MATERIALS AND METHODS

In this work, an automated helping tool inspired by the ABCD rule was established by using pre-processed and segmented dermoscopic images that are taken from the first publicly available dataset of dermoscopic images (called PH2 - Pedro Hispano hospital). The dataset was released by the team of ADDI/FCT project, which contains a total number of 200 melanocytic lesions, including 80 common nevi, 80 atypical nevi, and 40 Melanomas (Mendonca et al. 2013). The usage of MATLAB program to build the tool's algorithm was as the following:

A-Asymmetry Index (AI)

The Asymmetry feature takes a 'zero,' 'one,' or 'two' score depending on the asymmetry on both horizontal and vertical axes. The lesion makes a score 'zero' if it lacks asymmetry in both axes (fully symmetric), 'one' if it is asymmetrical in only one axis and 'two' if it is asymmetrical in two axes. The asymmetry index for each axis was calculated by taking the standard deviation among the different widths in the overlapped image. If the standard deviation value was higher than 22 pixels, then the asymmetry index for that lesion on this axis will be 'one.' If not, then the value will be 'zero.' **Fig. 2** represents the flowchart of the Asymmetry Index algorithm methodology.

B-Borders Irregularity Index (BII)

On the ABCD-rule, the lesion takes a score from 0-8 to assess the borders irregularity; to follow a series of steps calculated the rule the borders irregularity index of the lesion. First, the binary image of the segmented lesion was smoothed by the convolution with a Gaussian filter. Where the Gaussian filter, is the only convolution kernel or mask that does not produce any new irregularities, indentations, or protrusions, as artifacts during a continuous smoothing process (Atkins and Lee 2000). Then the borders of the two halves, which were resulted from the horizontal axis bisection, were handled as graphs of two different functions. Finally, the inflection points in the two halves were found and calculated to assess the borders' irregularity index. The inflection point indicates the point where the change in the graph concavity direction occurs. **Fig. 3** shows the flowchart of the Borders Irregularity Index algorithm methodology.

C-Colors Variation Index (CVI)

On the ABCD rule, the color criteria take a score from 1-6 depending on the number of colors in the tested skin lesion. The six main colors are White, Red, Light brown, Dark-brown, Blue-gray, and Black. To examine and extract the number of colors in the skin lesion, the Euclidian distance in the HSV color space was used on sequential steps. Initially, the RGB dermoscopic image of the whole lesion was multiplied by the binary image of the segmented lesion, to get only the lesion area on the RGB color space surrounded by a black background. The black background was converted to green since black was one of the colors that the system is looking for. After that, the dermoscopic image in the RGB color space was transformed into the HSV/HSL color space (Hue, Saturation, and Value or Lightness). Hue represents the color type that is described in terms of an angle ranging from 0°-360°. Although a circle contains

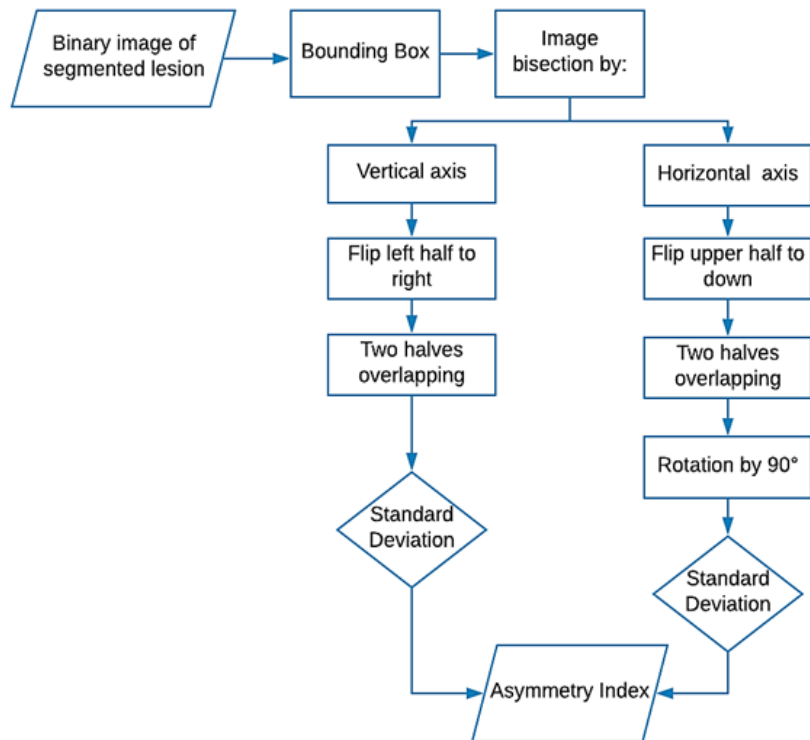


Fig. 2. Flowchart of Asymmetry Index algorithm methodology

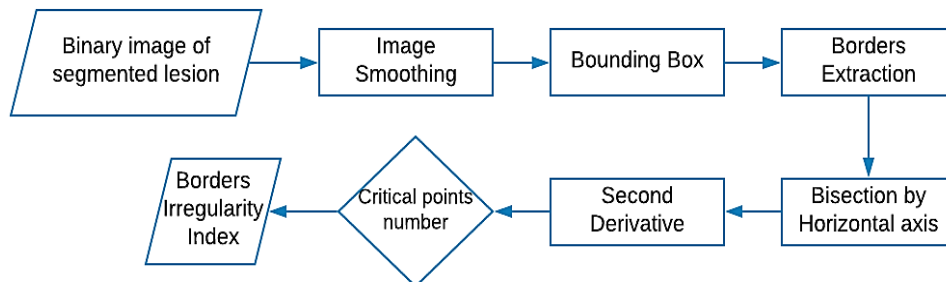


Fig. 3. Flowchart of Borders Irregularity Index algorithm methodology

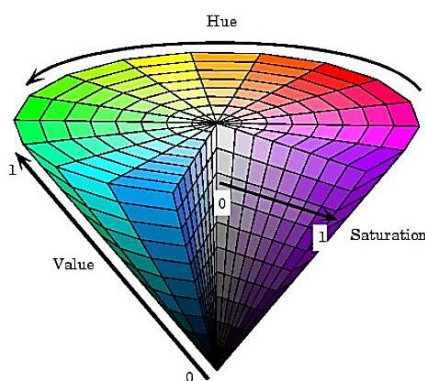


Fig. 4. HSV color space (Erdoğan and Yılmaz 2015)

360 degrees of rotation, the hue value is normalized to a range from 0 to 1. It changes from red to yellow, green, cyan, blue, magenta and again red. Saturation describes the vibrancy of the color. As it changes from 0 to 1, the lower the saturation value of the color, the grayer is present in color, causing it to appear faded. Value or

Lightness in the HSV expresses the brightness of the color. It ranges from 0 to 1, with 0 being completely dark and 1 being fully bright.

Fig. 4 shows the Hue, Saturation, and Value of the HSV color space. Where the hue is symbolized as a three-dimensional conical formation of the color wheel, the saturation is represented by the distance from the center of a circular cross-section of the cone, and the value is the distance from the pointed end of the cone (Erdoğan and Yılmaz 2015). The HSV color space was used because it is more related to human color perception, and it was chosen as the most efficient color space in skin detection in the face recognition systems (Chaves-gonzález et al. 2010). The conversion between the RGB and HSV color spaces was done using mathematical formulas as described in (Dong et al. 2018).

After the image was converted into the HSV color space, the desired six colors were identified in the system as fixed-points with specific values, as in **Table**

Table 2. RGB and HSV descriptions of ABCD colors (Lazaridis et al. 2007)

Colors	RGB(0-255)	HSV(0-1,0-1,0-1)	HSV (°, %, %)
White	255,255,255	0,0,1	0°,0%,100%
Red	255,0,0	0,1,1	0°,100%,100%
Light-brown	205,133,63	0.08,0.69,0.80	30°,69.30%,80.4%
Dark-brown	101,67,33	0.08,0.67,0.40	30°,67.30%,39.6%
Blue-gray	0,134,139	0.51,1,0.55	182°,100%,54.5%
Black	0,0,0	0,0,0	0°,0%,0%

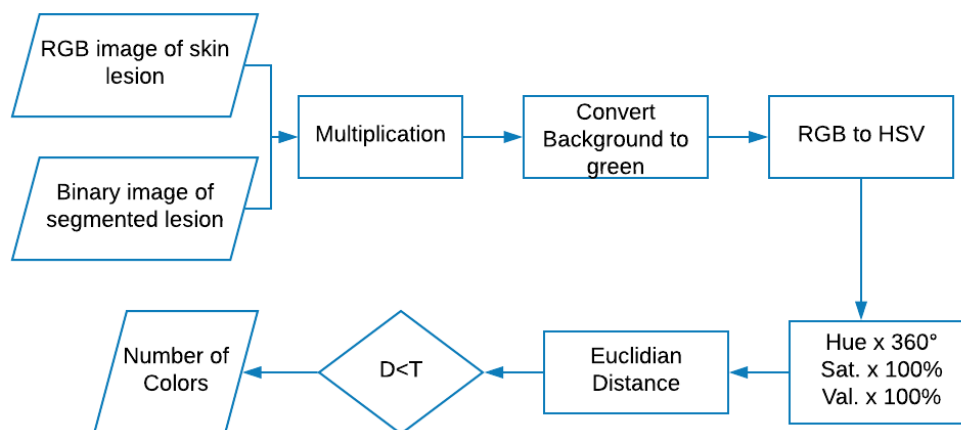


Fig. 5. Flowchart of Color Variation Index algorithm methodology

2. Then all the pixels in the tested lesion image are scanned, and the Euclidian distance (D) is calculated between their color and the six reference colors using the Euclidian distance equation (Eq.2) (Lazaridis et al. 2007). To overcome the square-root of decimal numbers and to get more accurate results, the hue channel was converted to 360° also the saturation and value channels were altered to 100%, as in the fourth column in **Table 2**.

$$D = \sqrt{(r - r1)^2 + (g - g1)^2 + (b - b1)^2} \quad (\text{Eq.2})$$

(Lazaridis et al. 2007)

Finally, to assess the number of colors, which are presented in the interested lesion a threshold, value for each color was determined. For White, Black, and Blue-gray colors, a threshold value (T) of 10 was used for the detection and a threshold value of 20 for Red, light-brown, and Dark-brown colors. If the tested pixel gave an Euclidian distance smaller than the determined threshold value of one of the reference colors (D < T) it is concluded that the pixel has that color or, more precisely, a “shade of it.” The exactness of color matching depends on the threshold value T. For smaller threshold values T we get more exact color matching. **Fig. 5** previews the flowchart of the color variation methodology.

D-Dermoscopic Structures Index (DSI)

Five main dermoscopic structures take place in the scoring system that includes; the presence of the network, homogenous areas, streaks, dots, and globules. Each can be detected based on different texture features such as completed local binary pattern (CLBP), gray-level co-occurrence matrix (GLCM), and Gabor filter. Related to the presence of the mentioned

structures based on the results of the texture features, the lesion will take a score in the TDS Equation from 1- 5.

RESULTS AND DISCUSSION

The 200-dermoscopic images in the PH2 database were analyzed using the Asymmetry Index, the Borders Irregularity Index, and the Color Variation Index algorithms. The database provides the manual segmentation and the clinical diagnosis of the skin lesion as well as the identification of other critical dermoscopic criteria for each image in the database. These dermoscopic criteria include the assessment of the lesion asymmetry, along with the identification of colors and several differential structures, such as pigment network, dots, globules, streaks, regression areas, and blue-whitish veil (Mendonc et al. 2013, Muchun et al. 2018).

Unfortunately, the D-Dermoscopic Structures Index algorithm was not accomplished due to time limitations. The results of the Asymmetry Index and the Color Variation Index were reported in terms of Sensitivity, Specificity, and Accuracy, using the following equations (Masood and Al-jumaily 2017):

$$Sensitivity = \frac{TP}{TP + FN} \times 100\% \quad (\text{Eq.3})$$

$$Specificity = \frac{TN}{TN + FP} \times 100\% \quad (\text{Eq.4})$$

$$Accuracy = \frac{TP + TN}{TP + TN + FP + FN} \times 100\% \quad (\text{Eq.5})$$

Sensitivity, or recall (SE), refers to the number of correctly identified cancer cases to the total number of cancer cases in the dataset. Specificity of true negative

Table 3. Sensitivity, Specificity & Accuracy for the Asymmetry Index algorithm at different Threshold values

Threshold	21	22	23	24	25	26
Sensitivity	81.48%	81.48%	78.52%	66.23%	73.33%	70.37%
Specificity	50.19%	52.83%	56.98%	57.72%	64.91%	67.17%
Accuracy	60.75%	62.50%	64.25%	61.00%	67.75%	68.25%

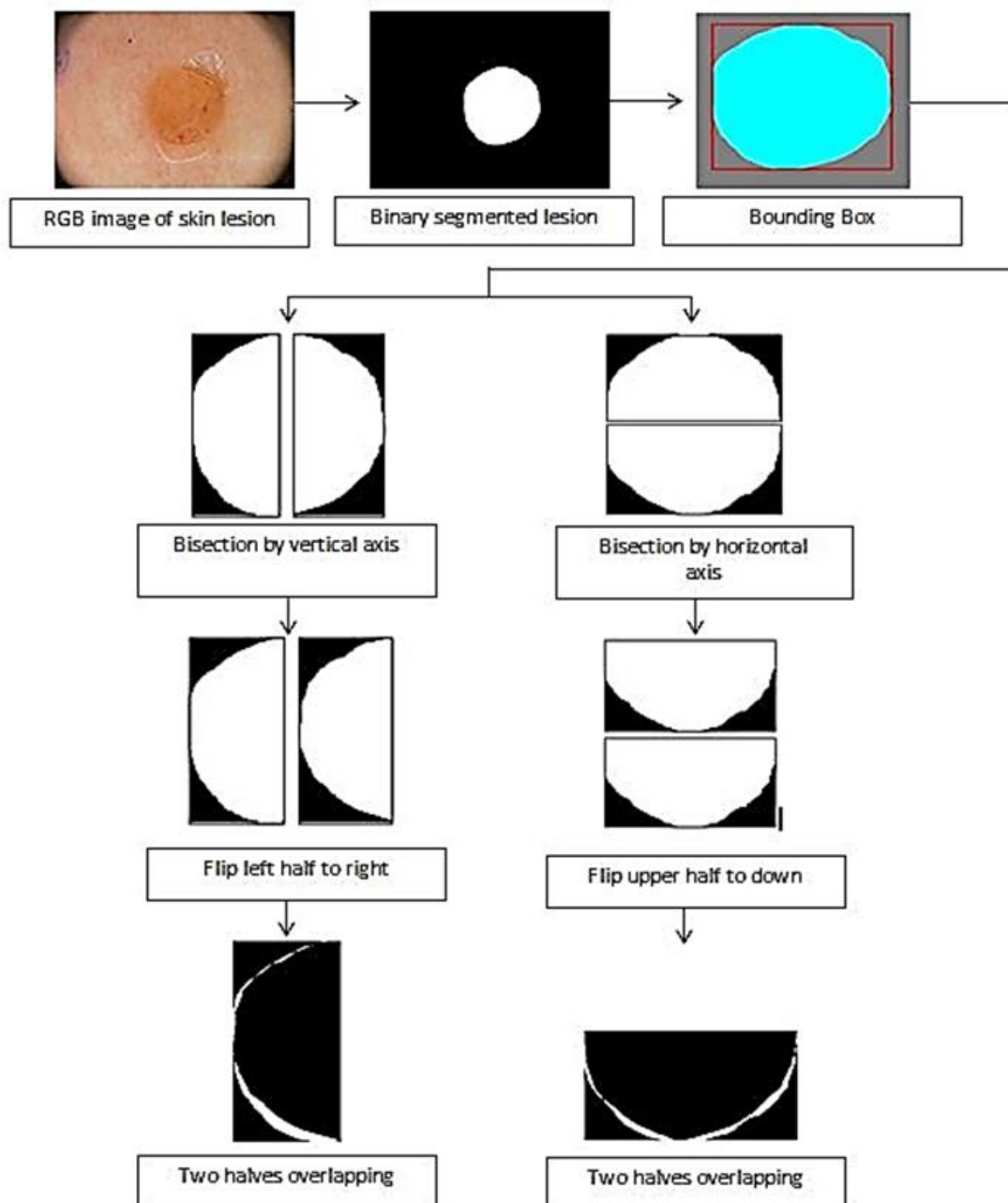


Fig. 6. The resulted images from the Asymmetry Index algorithm with '0' AI score result

rate (SP) refers to the number of correctly identified non-cancer cases to the total number of non-cancer cases in the dataset and accuracy refers to the proportion of both correctly identified cancer and non-cancer cases to the total number of both cases in the dataset.

A-Asymmetry Index (AI)

The Asymmetry Index Algorithm achieved a sensitivity of 81.48%, a specificity of 52.83%, and an

accuracy of 62.50% at threshold value equal to 22, as in **Table 3**. The threshold value was chosen based on the sensitivity value, considering the high sensitivity as the priority measure in all Melanoma or general cancer case classifications (Rastgoo et al. 2015).

Figs. 6-8 represent the resulted images from the Asymmetry Index algorithm step by step with '0', '1' & '2' final AI score, respectively.

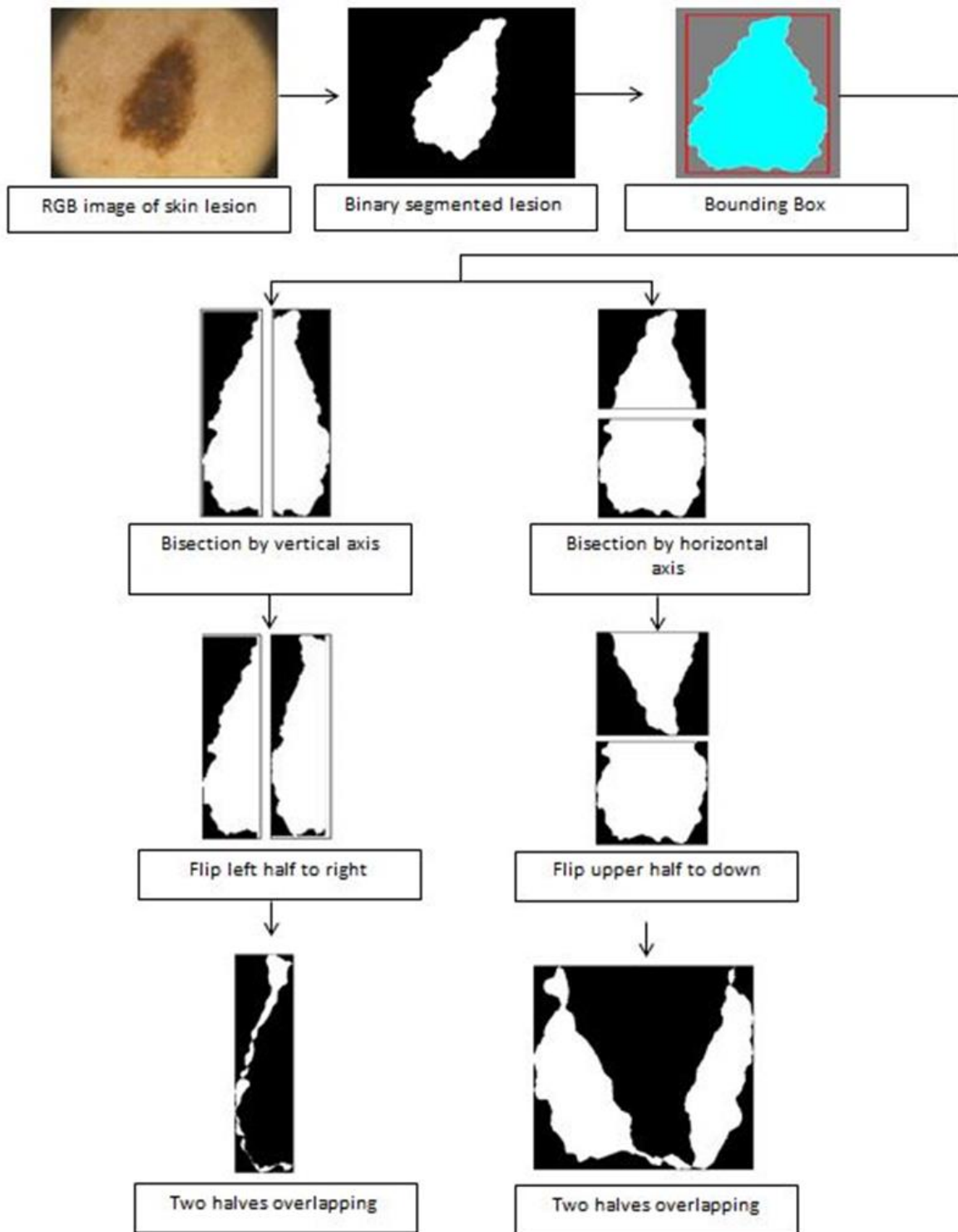


Fig. 7. The resulted images from Asymmetry Index algorithm with '1' AI score result

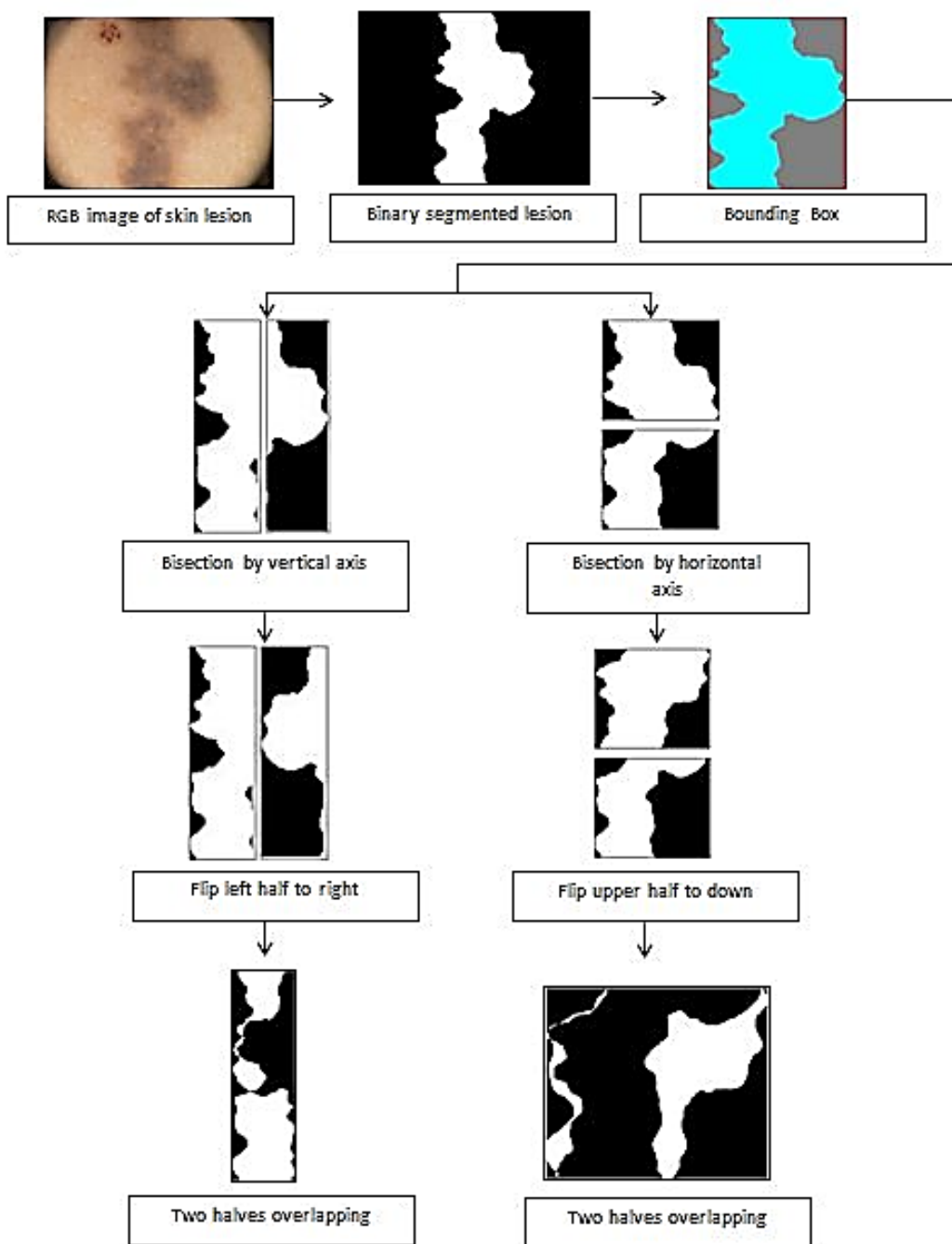


Fig. 8. The resulted images from Asymmetry Index algorithm with '2' AI score result

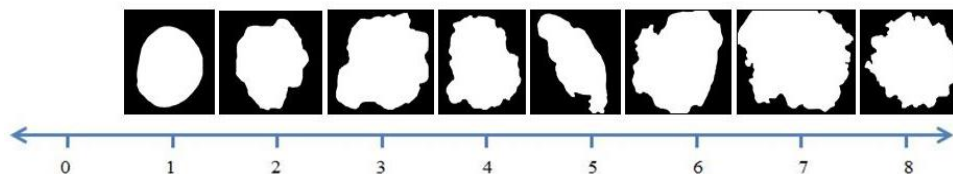


Fig. 9. Different skin lesions with borders irregularity index value vary from 1-8

B-Borders Irregularity Index (BII)

As mentioned before, the PH2 database does not offer any assessment of the borders irregularity for the dermoscopic images. Therefore, the Borders Irregularity

Index results were not reported as the results of other indices. So the results of the algorithm were represented giving a score from 0-8 based on the number of inflection points to assess the BII of a lesion, as in **Fig. 9**.

Table 4. Sensitivity, Specificity & Accuracy for the Color Variation Index at different Threshold values

Threshold	White	Red	Light-brown	Dark-brown	Black	Sensitivity	Specificity	Accuracy
1	20	20	20	20	20	52.19%	55.50%	54.30%
2	15	15	15	15	15	47.27%	63.25%	57.49%
3	10	10	10	10	10	38.25%	69.40%	58%
4	10	10	10	20	10	41.26%	62.93%	55%
5	15	15	15	20	15	47.81%	60.25%	55.70%
6	15	15	20	20	15	51.64%	59.78%	56.80%
7	15	20	20	20	15	51.91%	59.78%	56.90%
8	10	20	20	20	10	51.37%	61.51%	57.80%
9	10	10	20	20	10	51.10%	61.50%	57.70%

The Colors Variation Index algorithm achieved a sensitivity of 51.37%, a specificity of 61.51%, and accuracy of 57.80% in the detection of 5 colors out of 6 with different threshold values, as shown in **Table 4**. The detected *colors are White, Red, Light-brown, Dark-brown, and Black. The algorithm was not able to identify the Blue-gray color due to the difficulties to detect the center of this color numerically.

One of the factors that affect the results of the AI and the CVI algorithms was due to the inaccurate manual segmentation in the database.

CONCLUSIONS

This work created a computational tool based on the ABCD-rule, which is helpful for both experienced and non-experienced dermatologists in the early discrimination of Melanoma than other types of skin

lesions and to eliminate the need of the biopsy procedure. A new metric for the Borders Irregularity Index was established depending on the number of inflection points in the lesion's borders. Finally, the number of colors in the tested lesion was calculated from the Colors Variation Index algorithm based on the Euclidian distance. Future work for this project may include several points. First, to build an algorithm that can detect the presence of different dermoscopic structures, such as pigmented network, homogenous areas, streaks, dots, and globules. Another enhancement that could be made is to modify the tool to be able to pre-process and segment each dermoscopic input image. Finally, the tool can be enhanced by building a Graphical User Interface (GUI) system to make the tool more reliable and practical for clinicians and dermatologists use.

REFERENCES

- Argenziano G, Soyer HP, De Giorgi V, Piccolo D, Carli P, Delfino M, Ferrari A, et al. (2000) Interactive Atlas of Dermoscopy. EDRA Medical Publishing & New Media.
- Atkins MS, Lee TK (2000) A New Approach to Measure Border Irregularity for Melanocytic Lesions. (July 2017). <https://doi.org/10.1117/12.387728>
- Chaves-gonzález JM, Vega-rodríguez MA, Gómez-pulido JA, Sánchez-pérez JM (2010) Detecting Skin in Face Recognition Systems: A Colour Spaces Study. Digital Signal Processing 20(3): 806-823. <https://doi.org/10.1016/j.dsp.2009.10.008>
- Day GR, Barbour RH (2000) Automated Melanoma Diagnosis: Where Are We At? Skin Research and Technology 6(1): 1-5.
- Dong C, Liang G, Hu B, Yuan H, Jiang Y, Zhu H (2018) Prediction of Congou Black Tea Fermentation Quality Indices from Color Features Using Non-Linear Regression Methods. (June): 1-11. <https://doi.org/10.1038/s41598-018-28767-2>
- Erdoğan K, Yılmaz N (2015) Shifting Colors to Overcome Not Realizing Objects Problem Due to Color Vision Deficiency. (December 2014): 10-14. <https://doi.org/10.15224/978-1-63248-034-7-27>.
- Jain S, Jagtap V, Pise N (2015) Computer Aided Melanoma Skin Cancer Detection Using Image Processing. Procedia Computer Science 48(C): 736-741. <https://doi.org/10.1016/j.procs.2015.04.209>
- Lazaridis P, Zaharis ZD, Kampitaki DG (2007) Simple Matlab Tool for Automated Malignant Melanoma Diagnosis Simple Matlab Tool for Automated Malignant Melanoma Diagnosis. (December 2013).
- Loane M, Gore H, Corbett R, Steele K, Mathews C, Bloomer S, Eedy D, Telford R, Wootton R (1997) Effect of Camera Performance on Diagnostic Accuracy: Preliminary Results from the Northern Ireland Arms of the UK Multicentre Teledermatology Trial. Journal of Telemedicine and Telecare 3(2): 83-88.
- Masood A, Al-jumaily AA (2017) Computer Aided Diagnostic Support System for Skin Cancer: A Review of Techniques and Algorithms. International Journal of Biomedical Imaging 2013: 11-12.
- Mendonc T, Ferreira PM, Marques JS (2013) PH 2 - A Dermoscopic Image Database for Research and Benchmarking*: 5437-5440.

- Muchun W, Wenzhong Z, Siqi Z (2018) The Relationship Between Low-Carbon Finance and Sustainable Development: A Case Study of Industrial Bank of China. *International Journal of Sustainable Energy and Environmental Research*, 7(1): 24-34.
- Oliveira RB, Papa JP, Pereira AS, Tavares JMRS (2018) Computational Methods for Pigmented Skin Lesion Classification in Images: Review and Future Trends. *Neural Computing and Applications* 29(3): 613-636. <https://doi.org/10.1007/s00521-016-2482-6>
- Rastgoo M, Garcia R, Morel O, Marzani F (2015) Automatic Differentiation of Melanoma from Dysplastic Nevi. *Computerized Medical Imaging and Graphics* 43: 44-52. <https://doi.org/10.1016/j.compmedimag.2015.02.011>
- Stolz W, Riemann A, Cagnetta AB (1994) ABCD Rule of Dermatoscopy: A New Practical Method for Early Recognition of Malignant Melanoma. *European Journal of Dermatology* 4: 521-527.

www.ejobios.org